Biosensors and Bioelectronics 126 (2019) 261–268

Contents lists available at ScienceDirect

Biosensors and Bioelectronics

journal homepage: www.elsevier.com/locate/bios

# Aptamer-DNA concatamer-quantum dots based electrochemical biosensing strategy for green and ultrasensitive detection of tumor cells via mercury-free anodic stripping voltammetry

Yue Zheng[a,*], Xiaoyu Wang[b], Shengquan He[b], Zehua Gao[b], Ya Di[a], Kunling Lu[a], Kun Li[b], Jidong Wang[b,*]

[a] The First Hospital in Qinhuangdao Affiliated to Hebei Medical University, Qinhuangdao 066004, China
[b] Hebei Key Laboratory of Applied Chemistry, School of Environmental and Chemical Engineering, Yanshan University, Qinhuangdao 066004, China

ARTICLE INFO

*Keywords:*
Aptamer-DNA concatemer-CdTe Quantum dots
GR- PDDA/L- Cys composites
Mercury-free anodic stripping voltammetry
Tumor detection
Electrochemical biosensor

ABSTRACT

A electrochemical biosensing strategy was developed for green and ultrasensitive detection of tumor cells by combining aptamer-DNA concatamer-CdTe quantum dots (QDs) signal amplification probe with mercury-free anodic stripping voltammetry (ASV). First, aptamer-DNA concatamer- CdTe QDs probes were designed by DNA hybridization and covalent assembling, which contained specific recognition of aptamer and signal amplification incorporating the DNA concatamer with QDs. Meanwhile, the capture electrode, glassy carbon electrode (GCE)/ Graphene oxide (GO)/Polyaniline (PANI) / Glutaraldehyde (GA) / concanavalin A (Con A) was fabricated by a layer-by-layer assembling technique. K562 cells, as model cancer cells were detected to demonstrate the feasibility of this sensing strategy. Then, novel composite, graphene (GR)- Poly diallyldimethylammonium chloride (PDDA)/L-Cysteine (L- Cys), was explored in ASV which replaced mercury electrodes using for determination of tumor cells. The proposed electrochemical biosensor showed high sensitivity with the detection limit of 60 cells $mL^{-1}$. More importantly, this novel design of signal amplification probes and the exploration of new composites in mercury-free ASV analysis would provide a promising method for ultrasensitive biosensor preparation and green electrochemical detection of tumor cells.

## 1. Introduction

Sensitive and specific determination of tumor cells is essential in clinical cancer screening and disease diagnosis (Loren et al., 2013; Mullighan et al., 2008, 2009). Numerous typical detection methods have been developed including flow cytometry, polymerase chain reaction, and immunohistochemistry (Li et al., 2002; Liu et al., 2013; Pitsillides et al., 2011; Zhou et al., 2016a, 2016b; Phillips et al., 2009; Schamhart et al., 2003; Singh et al., 2004). Electrochemical biosensing detection, due to moderate cost, instrumental simplicity, and high sensitivity, has attracted worldwide attention (Grieshaber et al., 2008; Saha et al., 2012; Shao et al., 2010). To achieve higher sensitivity and selectivity, various new materials and novel designs have been explored in electrochemical biosensors construction, such as nanomaterials (Liu et al., 2016; Tu et al., 2015; Yang et al., 2018), conducting polymers (Rowe et al., 2011), aptamers (H. Liu et al., 2013; W. Liu et al., 2013) and catalyst enzymes (Zhu et al., 2011).

Quantum dots (QDs), as a new nanomaterial, due to their electroactivity (Gill et al., 2008; Liu et al., 2004), versatility in surface modification and unique optical properties (Wang et al., 2017; Cui et al., 2007; Qian et al., 2006; Zhang et al., 2006) have attracted more and more interests. Recently, QDs incorporating with a wide variety of DNA concatemer, as new amplifying tags, have been developed in electrochemical biosensor (Chen et al., 2011; Liu et al., 2013). Liu et al. (H. Liu et al., 2013; W. Liu et al., 2013) developed a versatile super-sandwich cytosensor for detecting cancer cells. They combined the signal amplification of the DNA concatemer, the specific binding ability of aptamer, the optical and electrical properties of QDs, with the sensitive detection of fluorescence and electrochemistry. Multiwall carbon nanotubes (MWCNTs) @ polydopamine (PDA)@Au QDs composites were assembled on the surface of the electrode as the immobilization matrices of concanavalin A (Con A) to capture tumor cells. Then, aptamer-DNA concatamer-CdTe QDs as signal probe bond specifically on the cells. These design strategies in biosensor exhibited good sensitivity, wide linear range ($1.0 \times 10^2$ to $1.0 \times 10^6$ cells $mL^{-1}$), good reproducibility and acceptable precision (The detection limit is estimated to be

* Corresponding authors.
*E-mail addresses:* yuezheng1965@sina.com (Y. Zheng), wangjidong@ysu.edu.cn (J. Wang).

https://doi.org/10.1016/j.bios.2018.09.076
Received 15 August 2018; Received in revised form 20 September 2018; Accepted 20 September 2018
Available online 21 September 2018
0956-5663/ 

50 cells $mL^{-1}$ at 3σ). Zhang et al. (Zhang et al., 2017) reported a new "signal-off" photoelectrochemical (PEC) immunosensor for detecting prostate specific antibody (PSA). The signal amplification resulted from the design of DNAzyme concatemer and hemin/G-quadruplex-assisted biocatalytic precipitation CdS:Mn/g-$C_3N_4$ nanohybrids. The photocurrent responses of this immunosensor using for detecting PSA also exhibited the lower detection limit (3.8 pg $mL^{-1}$), acceptable specificity and reproducibility. Thus, theses design strategies of signal amplification probes, combining the DNA concatemer, in which signal probes hybridized multiple target molecules (or multiple target regions of one molecule) to create long DNA concatamers, and QDs with electrochemical analysis would initiate new ideas for the biosensor construction. Anodic stripping voltammetry (ASV), as a most popular detection technique for heavy metal ions has been successfully combined with electrochemical biosensors using for detecting protein, thrombin and tumor cells (Daniele et al., 2003; Jie et al., 2014; Li et al., 2010). Mercury is the most widespread electrode material due to its wide potential window in the cathodic area, excellent stripping characters, the ease of renewing the electrode surface and high sensitivity (Economou and Fielden, 2003; Shen et al., 2013). However, for its dramatic toxicity, many researchers have tried to explore mercury-free electrodes using for determination of trace metals in stripping voltammetry analysis (Herzog and Arrigan, 2005; Honeychurch and Hart, 2003; Wang et al., 2000). Several new electrode materials including alternative liquid metal electrodes, bare solid electrodes, and film electrodes (Berduque et al., 2007; Di and Zhang, 2003; Surmann and Zeyat, 2005), have recently been reported. L- cysteine (L-Cys), as conducting polymers and widely available amino acid, could strongly adsorb on the surface of GCE (W. Liu et al., 2013; H. Liu et al., 2013). Such a layer should be a promising electrode material for sensing detection. Zhou et al. (Zhou et al., 2016a, 2016b) reported a novel electrochemical detection of $Cd^{2+}$ and $Pb^{2+}$ in milk based on L-Cys and graphene (GR) modified glassy carbon electrode. The electrochemical behaviors of $Cd^{2+}$ and $Pb^{2+}$ on the L-Cys/GR-chitosan (CS)/GCE electrode were studied by differential pulse anodic stripping voltammetry (DPASV). The oxidation peak current of $Cd^{2+}$ was linear with its concentration in the range of 0.56–67.2 μg/L. Excellent conductivity and catalytic performance of graphene promoted the electron transfer in process of $Cd^{2+}$ oxidation. Meanwhile L-Cys contained sulfur, nitrogen, and oxygen atom which was easy to coordinate with $Cd^{2+}$. Both could promote the signal enhancement so that the L-Cys/GR composite would be as a candidate to replace mercury in ASV for $Cd^{2+}$ analysis.

Herein, we developed a novel aptamer-DNA concatamer-CdTe QDs probe based electrochemical biosensing strategy for green and ultrasensitive determination of tumor cells via a mercury-free ASV route as Scheme 1 shown. First, aptamer-DNA concatamer-CdTe QDs were designed by DNA hybridization and covalent assembling, which contained both specific recognition of aptamer and signal amplification incorporating the DNA concatamer with QDs. Then, as the capture electrode, concanavalin A (Con A), Glutaraldehyde (GA), Polyaniline (PANI) and Graphene oxide (GO) were modified on the surface of GCE in sequence (denoted as GCE/GO/PANI/GA/Con A) by a layer-by-layer assembling technique. As a proof-of-concept, human chronic myelogenous leukemia cancer cells (K562 cells) were selected as model sample to demonstrate the feasibility of the electrochemical biosensing strategy. Finally, novel composites, GR and Poly diallyldimethylammonium chloride (PDDA) with the certain ratios, were explored in the modification of GCE (denoted as GR-PDDA). After L- Cys film formed on the modified electrode, the detecting electrode, denoted as GCE/ GR-PDDA/ L- Cys, was obtained, which would replace mercury ion to form amalgam for adsorbing $Cd^{2+}$ using for the detection of tumor cells in ASV analysis. The proposed strategy based on novel design of signal amplification probes and the exploration of new composites in mercury-free ASV approach, provided a promising method for biosensor preparation and electrochemical detection of tumor cells.

## 2. Experiment

### 2.1. Materials and reagents

Graphene oxide was synthesized by the Hummers method (Dimiev and Tour, 2014). Graphite, $H_2SO_4$, $KMnO_4$ were purchased from Sigma (St. Louis, MO, USA). Graphene was purchased from Nanjing Xianfeng Nanotech Co. Ltd. (Nanjing, China). K562 cells line was obtain from SincereLion Technology (beijing) Co. Ltd. and were cultivated according to the literature (Ge et al., 2015). Polyaniline was obtained from Alfa Aesar (China chemical co., Ltd). Con A was purchased from Sangon Biotech Co., Ltd (Shanghai, China). $CdCl_2$, sodium tellurite, sodium borohydride, 3-mercaptopropionic acid (MPA), PDDA, L-Cys, potassium chloride, calcium chloride, manganese chloride, bovine serum albumin (BSA), glutaraldehyde, nitric acid (65%), potassium ferrocyanide, sodium acetate, glacial acetic acid and phosphate buffer solution (PBS, 10 mM, pH = 7.2–7.4) were obtained from Aladdin science and technology (China) Co. All reagents were analytical grade without further purification.

DNA sequences were obtained from Sangon Biotech (Shanghai) Co. Ltd, and the sequences were presented as below:

ssDNA1: 5- AGATA GCCAC TCGTA TTCAT CACTG GACCG TTTTT G*G*G*G*G* − 3

ssDNA2: 5-TACGA GTGGC TATCT -TCGAT TCCTA -TACGA GTGGC TATCT -TCGAT TCCTA -TACGA GTGGC TATCT -TTTTT TTTTT ACAGC AGATC AGTCT ATCTT CTCCT GATGG GTTCC TATTT ATAGG TGAAG CTGT − 3

ssDNA3 : 5- G*G*G*G*G* GAAAA ATTTT TTTTT TACAG CAGAT CAGTC TATCT TCTCC TGATG GGTTC CTATT TATAG GTGAA GCTGT − 3

(* indicate phosphorothioate linkage)

### 2.2. Apparatus

Scanning electron microscopy (SEM) images of the electrode surface were obtained with a SUPRA 55 SEM (CarlZeiss, Germany, operated at 10 kV). Transmission electron microscopic (TEM) images were obtained by a HT7700 TEM (Hitachi, Tokyo, Japan). UV–vis spectrometry was performed on UV-2450 (Shimazu, Japan) and fluorescence spectrum measurements were recorded on F-7000 (Hitachi, Tokyo, Japan). All electrochemical measurements were performed on a model CHI660E station (Chenhua Inc., Shanghai). Fluorescence microscopic image was obtained from XSP-63X fluorescence microscope (The first factory of optical instrument in Shanghai, China)

### 2.3. Preparation of aptamer-DNA concatamer- CdTe QDs probe

Synthesis of ssDNA1-CdTe QDs. The synthesis of ssDNA1-CdTe QDs via a one-pot route was according to literature procedures (Ma et al., 2008; Wang et al., 2018a, 2018b). Two different domains were designed in ssDNA1, that is, phosphorothioates (*ps*) backbone served as a ligand structure for the synthesis of QDs and phosphates (*po*) backbone in which the corresponding DNA sequence was used for hybridization with signal amplification regions of aptamer-DNA substrate strand (ssDNA2). As shown in 2.1, ssDNA2 contained one aptamer DNA sequence using for the specific recognition of tumor cells and three ssDNA1 target recognition units for signal amplification. For a typical synthesis, 0.2 mmol cadmium chloride, 0.2 mmol MPA, 25 mL distilled water were added into a three-necked flask in sequence under vigorous stirring. After pH was adjusted to 9.0 slowly with 1 M NaOH, 0.025 mmol sodium tellurite and 0.5 mmol sodium borohydride mixed with the above solution under the stirring at room temperature. Then, 10 μL ssDNA1 (10 μM) solution was added in 990 μL above mixture solution and heated to 90 °C for 2 h. The whole system was naturally cooled down to room temperature. After being wished three times with absolute ethanol and distilled water alternately, the ssDNA1- CdTe QDs

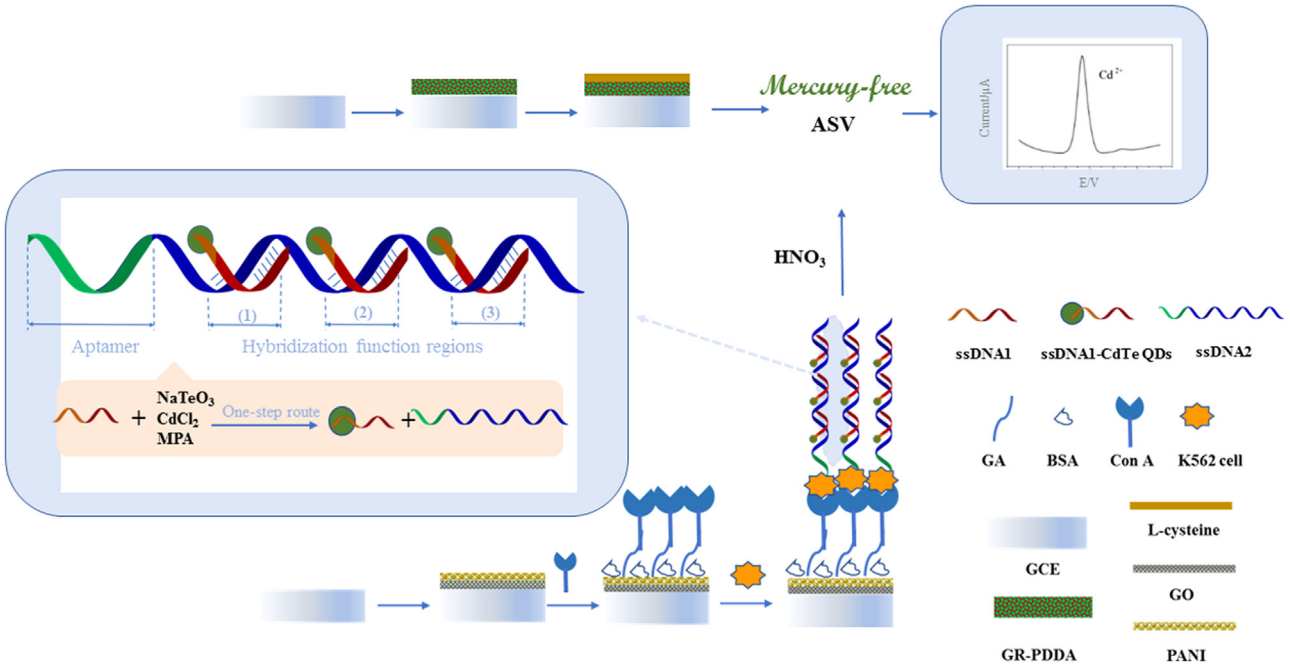


**Scheme 1.** Procedures for the fabrication of supersandwich cytosensor using controlled aptamer-DNA concatamer-QDs and the detection of $Cd^{2+}$ via a mercury-free ASV route.

were dispersed in PBS and stored in dark at 4 °C.

Synthesis of ssDNA3- CdTe QDs. The synthesis of ssDNA3 - CdTe QDs was also according the procedures of ssDNA1- CdTe QDs. Two different domains were designed in ssDNA3, that is, phosphorothioates backbone served as a ligand structure for the synthesis of CdTe QDs and phosphates backbone in which the corresponding DNA sequence was in accord with aptamer DNA sequence.

Preparation of aptamer-DNA concatamer- CdTe QDs. Typically, 0.2 mmol cadmium chloride, 0.2 mmol MPA, 25 mL distilled water were loaded into a three-necked flask in sequence under vigorous stirring. 0.025 mmol sodium tellurite and 0.5 mmol sodium borohydride were mixed in the above solution under the stirring(pH = 9) at room temperature. Then, 10 μL ssDNA1 (10 μM) solution was added in 990 μL above mixture solution and heated to 90 °C for 2.5 h. 10 μL ssDNA2 (1 μM) and 1 mL ssDNA1- CdTe QDs solution were mixed and heated to 95 °C for 10 min to make the folded ss- DNA chain spread out and then cooled down in ice-water bath. Then ssDNA1- CdTe QDs was assembled onto the ssDNA2 substrate strand and formed DNA superstructure. The mixture was then subjected to ultrafiltration using a 100 kDa MW filter. The aptamer-DNA concatame-CdTe QDs were obtained and stored in dark at 4 °C.

Cell culture. Human leukemia K562 cells were cultured in a flask with a RPMI 1640 medium (Gibco, Grand Island, NY) supplemented with 10% fetal calf serum, ciprofloxacin (10 μg $mL^{-1}$), in an incubator (5% $CO_2$, 37 °C). Cell counting was used by trypan dye exclusion method by a Neubauer's chamber (10 μL of cell suspension mixed with 10 μL of dye). The remaining cells in suspension were then centrifuged at 1100 rpm for 10 min and then suspended in sterile PBS buffer (pH = 7.4) (Gulati et al., 2018).

Confocal Microscopy Imaging. K562 cells ($1 \times 10^5$ cells $mL^{-1}$) were seeded onto a well plate. After 24 h, cells were incubated with aptamer-DNA concatamer- CdTe QDs probe for 1.5 h. To remove the unbound probes, the cells were washed three times with PBS. Then, the well was placed above a 20 × objective on the confocal microscope.

### 2.4. Fabrication of electrochemical biosensor

The fabrication and detection procedure of electrochemical biosensor were indicated in Scheme 1. The capture electrode GCE/GO/PANI/GA/Con A was prepared according to our recent work (Wang et al., 2018a, 2018b). More informations about the protocol were described in the Supporting information. The capture electrode GCE/GO/PANI/GA/Con A was immersed in K562 cells solution with different concentration at 37 °C for 30 min. After carefully washing with the buffer to remove non-captured cells, 5 μL aptamer- DNA concatamer-CdTe QDs probe solution was dropped onto the capture electrode and incubated at 37 °C for 1.5 h. The supersandwich biosensor were obtained (denoted as GCE/GO/PANI/GA/Con A/K562 cells/ aptamer-DNA concatamer-CdTe QDs). After rinsing with PBS, the biosensor was stored at dark stored in dark at 4 °C.

### 2.5. Construction of detecting electrode GCE/ GR- PDDA/ L-Cys and electrochemical analysis

Construction of detecting electrode GCE/ GR- PDDA/ L-Cys. Prior to surface modification, the GCE (d = 3 mm) was polished (0.05 mm alumina) and followed by successive sonication in acetone, $HNO_3$ (1:1 v/v), and distilled water, respectively. 5 μL mixture solution containing GR (100 μL, 1 mg $mL^{-1}$) and PDDA (6 μL, 20%) with different molar ratio was dropped on bare GCE and dried at room temperature for 2 h. The modified electrode, GCE/ GR–PDDA, was performed in 10 mmol $L^{-1}$ PBS (pH = 7.2) containing 1 mmol $L^{-1}$ L-Cys by CV scanning between −0.6 and 2.5 V for about 20 segments (scan rate, 100 mV $s^{-1}$).

Electrochemical analysis. To release $Cd^{2+}$, the obtained sensing system, GCE/GO/PANI/GA/Con A/K562 cells/ aptamer-DNA concatamer-CdTe QDs, was immersed in $HNO_3$ solution (200 μL, 0.1 M) for 2 h to dissolve the residual QDs. Then, 4.8 mL HAc-NaAc buffer (0.2 M, pH = 5.2) was added as the reaction supporting solution of ASV. The anodic stripping voltammetry detection involved electrodeposition at −1.2 V for 30 min, and stripping from −1.1 to −0.4 V using a square-wave voltammetry, with 4 mV potential steps, 25 Hz frequency and 25 mV amplitude. The oxidation peak of $Cd^{2+}$ was achieved at −0.86 V in ASV and the intensity of oxidation peak currents of $Cd^{2+}$ was proportional to the amount of K562 cells.

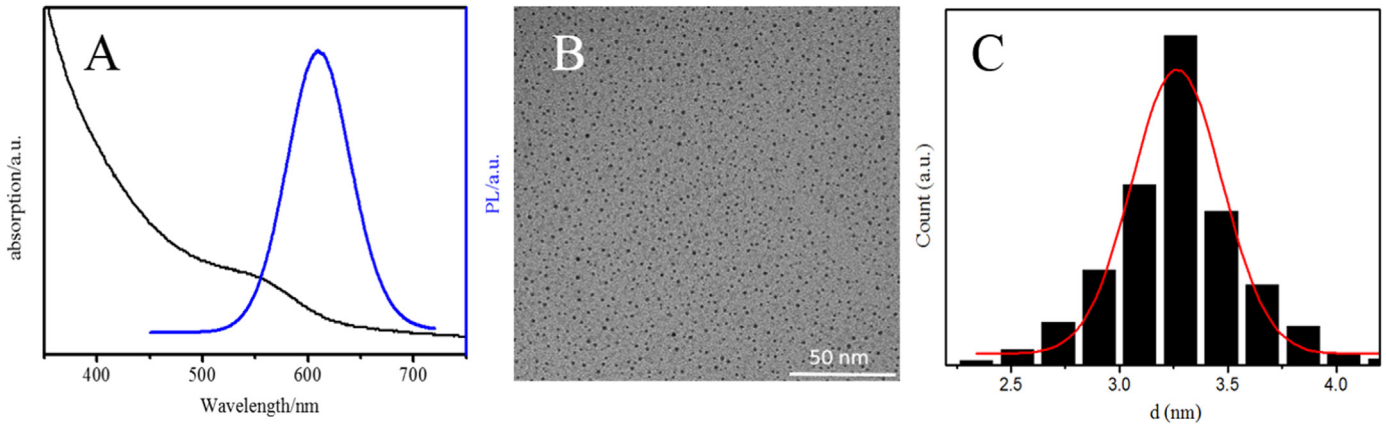


**Fig. 1.** UV–Vis and PL spectrum of DNA-CdTe QDs (A), TEM images (B) and particle size distribution histogram (C).

## 3. Results and discussion

### 3.1. Characterization of ssDNA1-CdTe QDs

ssDNA1-CdTe QDs were synthesized via a facile one-step route. The UV–vis absorption and PL spectra of ssDNA1- CdTe QDs were showed in Fig. 1A. A strong exciton absorption peak of ssDNA1- CdTe QDs appeared at 556 nm. The sharp PL emission peak was at about 609 nm and the full width at half maximum (FWHM) was about 26 nm, which represented CdTe QDs with a narrow size distribution. Furthermore, about 53 nm Nonresonant Stokes Shift (NRSS), which was the difference between positions of the band maxima of the absorption and emission spectra, indicated the CdTe QDs with the well-defined structure and minimum surface defects. According to the Peng's empirical formula (Yu et al., 2004): $D = (9.8127 \times 10^{-7})\lambda^3 - (1.7147 \times -10^{-3})\lambda^2 + (1.0064)\lambda - (194.84)$, the size of CdTe QDs was about 3.3 nm by the calculation, $D$ (nm) is the diameter of QDs and $\lambda$ (nm) is the excitonic absorption peak position. The TEM picture and the particle size distribution histogram support this conclusion as shown in Fig. 1B and C.

### 3.2. Characterization of aptamer- DNA concatamer -CdTe QDs probe

To investigate the effect of both the structure and number of QDs on signal intensity of aptamer- DNA concatamer -CdTe QDs probe, ssDNA3-CdTe QDs and aptamer- DNA concatamer -CdTe QDs probes were synthesized. A multifunctional ssDNA substrate (ssDNA2) was designed, which was comprised of the aptamer region to recognize K562 cell and three target regions to hybridize ssDNA1- CdTe QDs. After three ssDNA1-CdTe QDs had hybridized with DNA substrate (ssDNA2), the controlled aptamer- DNA concatamer -CdTe QDs probes were formed. The gel electrophoresis was also used to verify the formation of aptamer- DNA concatamer-CdTe QDs. In Fig. S1., ssDNA1, and ssDNA2 produced the bands at about 75 bp and 130 bp, respectively. Aptamer- DNA concatemer -CdTe QDs produced one band at above 300 bp. The results showed that aptamer- DNA concatamer -CdTe QDs had long DNA strands, and the hybridization reaction was implemented by ssDNA1, and ssDNA2. In order to ensure that the connection between tumor cells and probes, the two sample cells were incubated with the aptamer- DNA concatamer- CdTe QDs probe and ssDNA3-CdTe QDs probe at 37 °C for 2 h, respectively. The extracellular ssDNA3-CdTe QDs probes exhibited fluorescence image compared with the image under visible light irradiation, which suggested that the probes had bonded with K562 cells. The ssDNA3-CdTe QDs probe and aptamer-DNA concatamer- CdTe QDs probes experiments were carried out (Fig. 2A, Fig. 2B, Fig. 2C, Fig. 2D) and much stronger fluorescence intensity than ssDNA3-CdTe QDs probe at the equal reaction conditions which illustrated that aptamer- DNA concatamer- CdTe QDs probes were more effective in tumor cell detection. Thus, from what had discussed as above, we could control number and precise structure in probes by the design of target region in DNA substrate strand, and then regulated the signal intensity in electrochemical detection. The morphology and size of the probes were characterized by TEM as shown in Fig. 2E and Fig. 2F. The ssDNA3-CdTe QDs was nearly monodisperse and spherical, whose size was about 3 nm. And the aptamer- DNA concatamer- CdTe QDs probe showed a dendrimer- like structure about 10 nm.

### 3.3. Characterization of capture electrode GCE/GO/PANI/GA/Con A

The electrochemical impedance spectroscopy (EIS) and cyclic voltammetry (CV), as the effective tools, were adopted to investigate the assembly process of biosensor as shown in Fig. S2. The semicircle diameter of EIS in high frequency region is correlation to electron-transfer resistance ($R_{et}$). A change in diameter reflects the blocking behavior in the modification processes of electrode which associated with a change of $R_{et}$. (Pan et al., 2010). The $R_{et}$ of bare GCE showed a small value (Fig. S2A curve a) due to the free electron transfer process, and the peak current of CV was distinct (Fig. S2B curve a). while the GO modified electrode has a much higher $R_{et}$ in the ESI (Fig. S2A curve b), and the peak current of CV decreased (Fig. S2B curve b). But when the PANI modified electrode had a lower resistance (Fig. S2A curve c) and a higher the peak current of CV (Fig. S2B curve c), which proved that PANI was an excellent conducting material. Subsequently, the immobilization of GA and Con A onto the GCE/GO/PANI electrode, the resistance increased (Fig. S2A curve d,e), and the peak current of CV decreased continuatively( Fig. S2B curve d,e) which suggested that GA and Con A were immobilized on the electrode and blocked electron transfer between the redox probe and electrode. After capture of the K562 cells, the resistance showed great increase due to the dielectric behavior of cells. As expected, the peak current of CV further decreased (Fig. S2B curves f). Additionally, after incubation with aptamer DNA concatamer-QDs probes, the electrode was further hindered (Fig. S2A curve g and Fig. S2B curve g), which also suggested the capture electrode, GCE/GO/PANI/GA/Con A could capture the tumor cells and signal probes with high efficiency.

### 3.4. Characterization of detecting electrode and optimization of experimental conditions

The detecting electrode was needed to establish for achieving a novel non-toxic determination strategy, in which a GR- PDDA /L- Cys composites were explored. Abundant sulfur, nitrogen and oxygen elements in L- Cys could produce extremely strong adsorption for heavy metal ions such as $Cd^{2+}$ and $Pb^{2+}$ in the solution which could take the place of the amalgam in ASV process. To investigate the modified

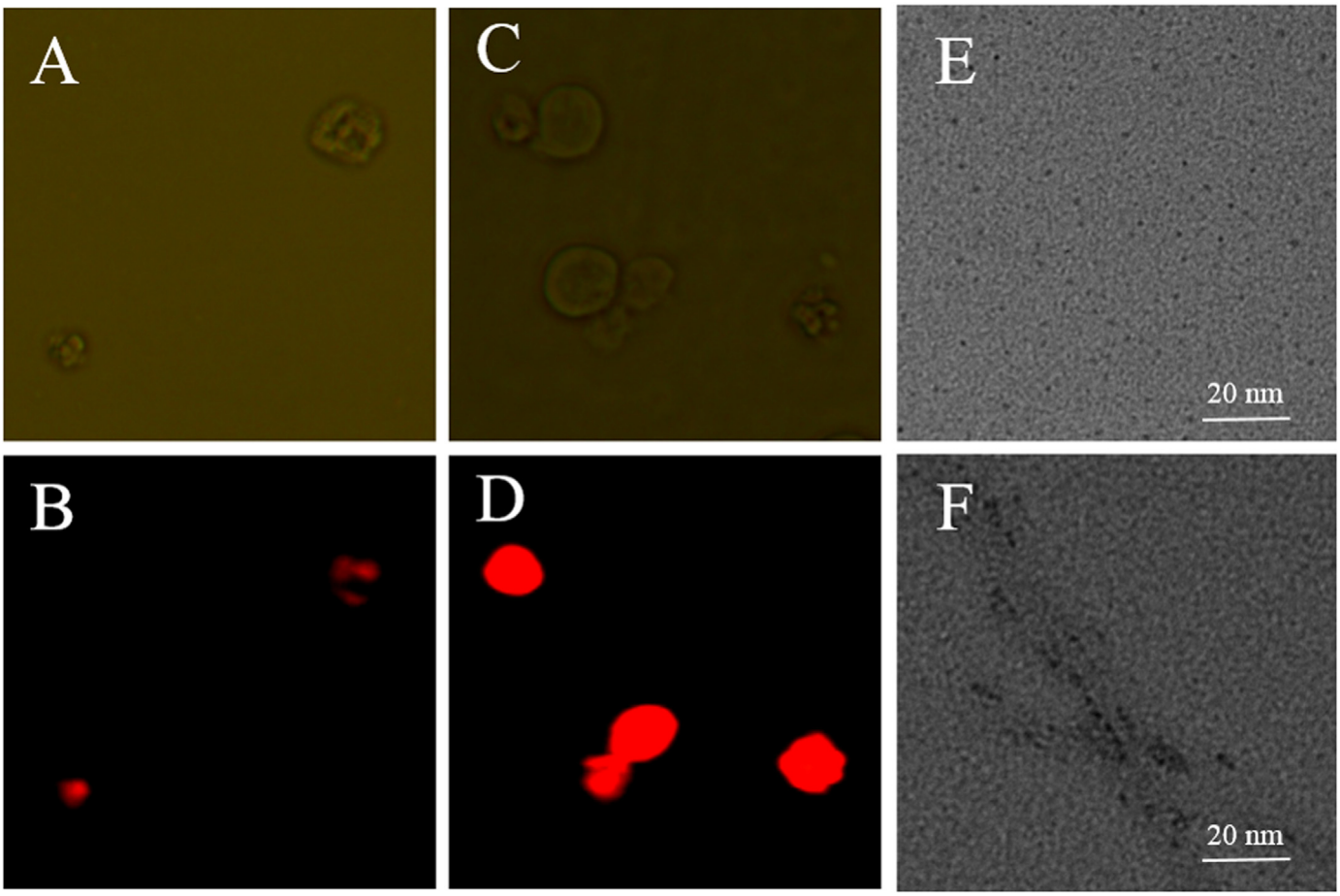


**Fig. 2.** Fluorescence microscopic images of single probe bonded K562 cells under visible light irradiation (A), and ultraviolet light irradiation (B). Fluorescence microscopic images of triploid probe bonded K562 cells under visible light irradiation (C), and ultraviolet light irradiation (D); TEM of aptamer-single DNA-QDs probes (ssDNA3-CdTe QDs) (E) and aptamer-DNA concatamer-CdTe QDs (F).

electrodes, EIS was used at the potential of 0.2 V under the participation of the redox reaction of $K_3Fe(CN)_6$/ $K_4Fe(CN)_6$ as shown in Fig. 3A. The semi-circle of EIS at high frequency region of bare GCE, GCE/ GR- PDDA and GCE/ GR- PDDA/ L- Cys increased which indicated the electronic transmission resistance of electrode interface grew gradually. This series of changes indicated that L- Cys and GR- PDDA were successfully modified on the bare GCE. Moreover, SEM images of the GCE/ GR- PDDA and GCE/ GR- PDDA/ L- Cys were shown in Fig. S3C. When GR- PDDA composites were assembled onto the GCE (Fig. S3C(A)), many particles appeared on the smooth surface of GCE, which illustrated that GR- PDDA had connected with GCE. After L-Cys being assembled, the SEM image of L-Cys coated GCE / GR- PDDA, became blurring and smooth, due to the form of the membrane resulted from the condensation reaction between L-Cys and GR- PDDA. The investigation of TEM also verified the assembly process of detecting electrode.

To optimize detecting electrode, GCE/ GR- PDDA/ L- Cys, electrochemical response, the effect of GR and PDDA with different ratio by $R_{et}$ and oxidation peak current was discussed. Like the adhesive, PDDA with positively charge made the completely incompatible GR load on the GCE surface. Different proportions between GR and PDDA impacted electronic transmission capability of electrode interface enormously. $R_{et}$ enhanced with the ratio value of GR: PDDA increasing (as Fig. 3B). Meanwhile, the ASV oxidation peak current increased with the ratio between GR and PDDA up from 1:1 to 1:3, and then down as shown in Fig. 3C and Fig. 3D. With the addition of PDDA, though a little PDDA could increase the specific surface area of the electrode by capturing much more signal recognition material, excessive PPDA also could make the electron transfer efficiency weak and signal intensity low. Thus, 1:3 was chosen as the optimized composite ratio between GR and PDDA.

### 3.5. Detection of K562 tumor cells

To prepare electrochemical biosensor, Con A was introduced to GCE, which was modified by GO and PANI composite through the crosslinking of GA as Scheme 1. Then, K562 cells were immobilized on the capture electrode, GCE/GO/PANI/GA/Con A, after BSA blocking the non- specific binding sites. Subsequently, aptamer- DNA concatemer -CdTe QDs probe (or ssDNA3-CdTe QDs probe) was captured on the surface of K562 cells and the supersandwich electrochemical biosensor was obtained. After GCE/GO/PANI/GA/Con A/K562 cells/aptamer-DNA concatemer -QDs probes were dissolved in $HNO_3$ solution, $Cd^{2+}$ could be released in the solution and detected by ASV. Due to much O, N, S of L- Cys resulted from GCE surface, the $Cd^{2+}$ ions were captured specifically at about $-0.86$ V. Compared with the conventional ASV peak position at $-0.72$ V (Zhou et al., 2016a, 2016b), the peak position migration occurred toward the negative potential direction because some materials such as GR, PDDA and L- Cys were adopted on the surface of GCE. The ASV response signal of this biosensor with different concentrations of K562 cells were shown in Fig. 4A. The intensity of peak currents of $Cd^{2+}$ showed a good linear relationship with the logarithm of cells concentration in range from $1.0 \times 10^2$ to $1.0 \times 10^7$ cells $mL^{-1}$ (Fig. 4B). The linear regression equation was $I = -4.82451 + 4.27868$ lg C, with a correlation coefficient of 0.9986 (n = 5). The limit of detection was 60 cells $mL^{-1}$ (S/N = 3).

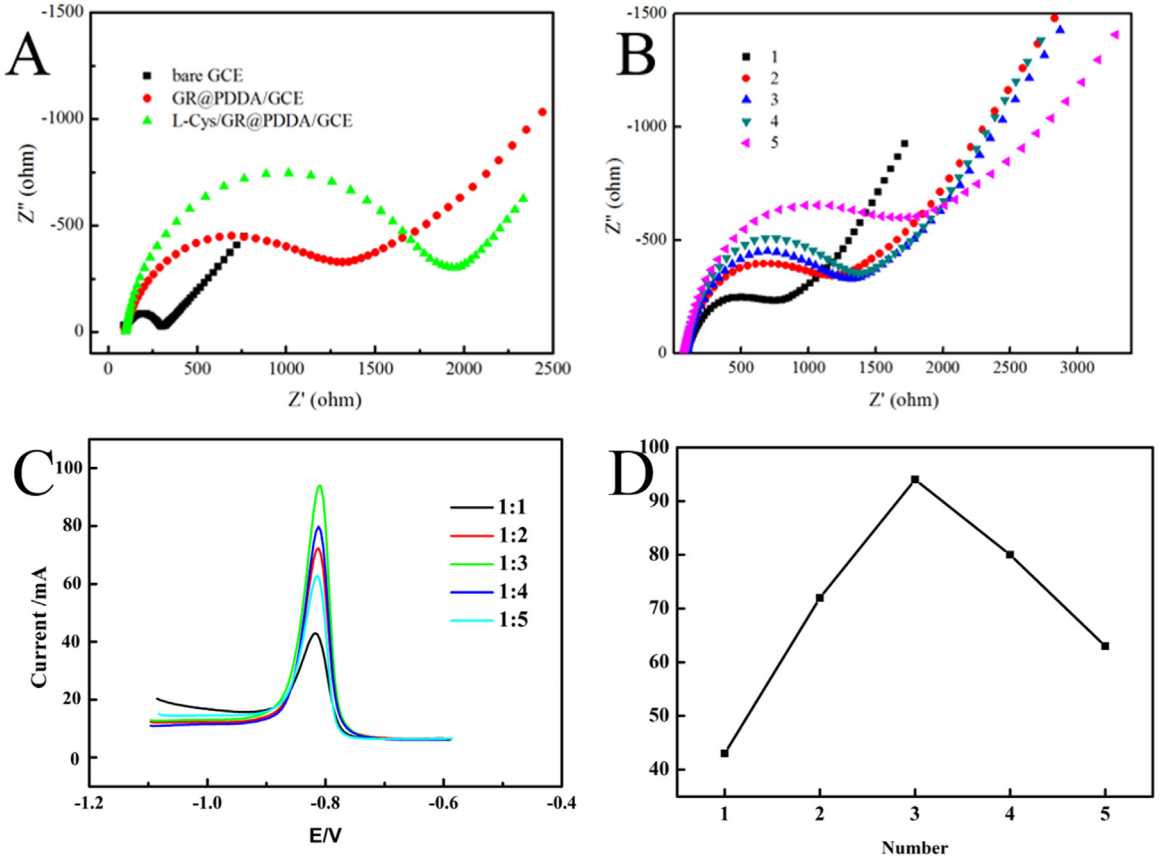


**Fig. 3.** EIS of bare GCE, GCE/GR-PDDA, GCE/GR-PDDA/L-Cys electrodes(A), and the EIS (B) and ASV (C), (D) of different proportion between GR and PDDA (Sample 1–5 were 1:1, 1:2, 1:3, 1:4, 1:5).

Furthermore, the single probe, ssDNA3-CdTe QDs, was also applied in the same experiment conditions (Fig. 4C) and the sensitivity of aptamer- DNA concatemer- CdTe QDs probe exhibited the superiority in analytical performance.

### 3.6. Selectivity and stability of the fabricated electrochemical biosensor

To examine the selectivity of this electrochemical biosensing system, HeLa cells and colorectal cancer cells were determined in the same detection conditions with $1.0 \times 10^5$ cells $mL^{-1}$. The electrochemical signals of HeLa cells and Hct116 cells were far lower than K562 tumor cells (Fig. 5), which illustrated our biosensor was with high specificity. To assess the reproducibility of electrochemical biosensor, three different concentrations of K562 cells including $1.0 \times 10^2$, $1.0 \times 10^3$ and $1.0 \times 10^4$ cells $mL^{-1}$ were investigated. The relative standard deviation (RSD) of these three assays were 7.22%, 5.26% and 5.76%, respectively, which meant that electrochemical biosensor with good reproducibility.

## 4. Conclusions

In summary, a novel electrochemical biosensor for detecting tumor cells was proposed using the aptamer- DNA concatamer- CdTe QDs signal amplification probes and new electrode modification composites, GR- PDDA /L- Cys, in mercury-free ASV for detecting $Cd^{2+}$. This green and controllably amplified electrochemical biosensor displayed good

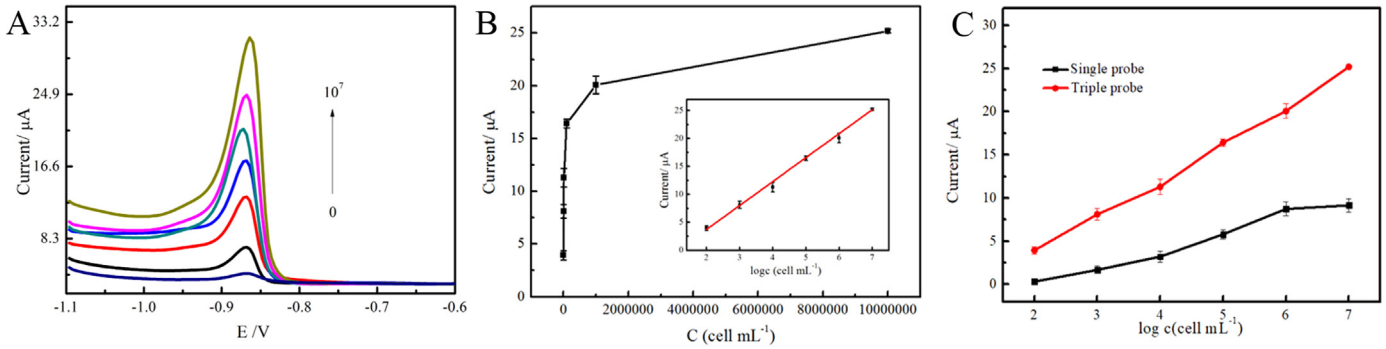


**Fig. 4.** (A) ASV of the electrochemical biosensor incubated with different concentrations of K562 cells: 0,$10^2$, $10^3$, $10^4$, $10^5$, $10^6$ and $10^7$ cells $mL^{-1}$. (B) The relationship of electrochemical signal and cell concentration. The range of K562 cell concentration is from $10^2$ to $10^7$ cells $mL^{-1}$. The illustrated error bars represent the standard error of three independent measurements. (C) The ASV performance comparison of aptamer-DNA concatamer-CdTe QDs probe and single probe (ssDNA3-CdTe QDs).

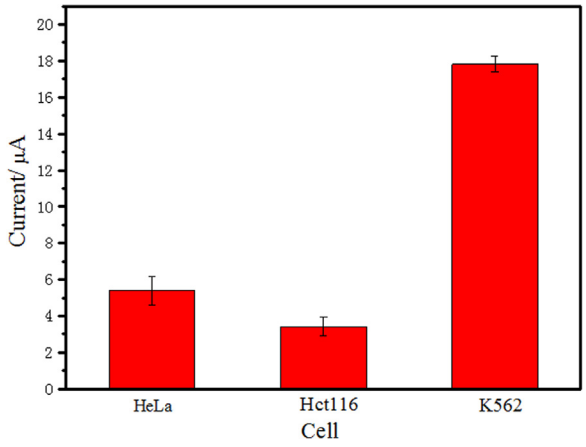


**Fig. 5.** Electrochemical signal of different tumor cells.

sensitivity, selectivity, wide linear range ($1.0 \times 10^2$ to $1.0 \times 10^7$ cells $mL^{-1}$) and acceptable precision (LOD was 60 cells $mL^{-1}$ (S/N = 3) for K562 cells). This design of signal amplification probes and the exploration of new composites would provide a promising method using for ultrasensitive biosensor preparation and green electrochemical detection of tumor cells.

## Acknowledgments

This research was supported by the Natural Science Foundation of Hebei Province (H2015203231), Youth Foundation Project supported by the Hebei Education Department of China (QN2014004), the Key Research and Development Program of Qin Huang Dao (201602A110), Doctoral Fund of Yanshan University (B821), Hebei Province Key Research and Development Projects(17272402D).

## Appendix A. Supporting information

Supplementary data associated with this article can be found in the online version at doi:10.1016/j.bios.2018.09.076.

## References

Berduque, A., Lanyon, Y.H., Beni, V., Herzog, G., Watson, Y.E., Rodgers, K., Stam, F., Alderman, J., Arrigan, D.W.M., 2007. Voltammetric characterisation of silicon-based microelectrode arrays and their application to mercury-free stripping voltammetry of copper ions. Talanta 71 (3), 1022–1030.

Chen, X., Lin, Y.-H., Li, J., Lin, L.-S., Chen, G.-N., Yang, H.-H., 2011. A simple and ultrasensitive electrochemical DNA biosensor based on DNA concatamers. Chem. Commun. 47 (44), 12116–12118.

Daniele, S., Ciani, I., Bragato, C., Baldo, M.A., 2003. Detection of heavy metals released at the sediment/water interface by combining anodic stripping voltammetry (ASV) and scanning electrochemical microscopy (SECM) measurements. J. De. Phys. 107, 353–356.

Di, J., Zhang, F., 2003. Voltammetry determination of trace manganese with pretreatment glassy carbon electrode by linear sweep voltammetry. Talanta 60 (1), 31–36.

Dimiev, A.M., Tour, J.M., 2014. Mechanism of Graphene Oxide Formation. ACS Nano 8 (3), 3060–3068.

Economou, A., Fielden, P.R., 2003. Mercury film electrodes: developments, trends and potentialities for electroanalysis. Analyst 128 (3), 205–212.

Ge, L., Su, M., Gao, C.M., Tao, X.T., Ge, S.G., 2015. Application of Au cage/Ru(bpy)(3)(2+) nanostructures for the electrochemiluminescence detection of K562 cancer cells based on aptamer. Sens. Actuators B-Chem. 214, 144–151.

Gill, R., Zayats, M., Willner, I., 2008. Semiconductor quantum dots for bioanalysis. Angew. Chem. Int. Ed. 47 (40), 7602–7625.

Grieshaber, D., MacKenzie, R., Voros, J., Reimhult, E., 2008. Electrochemical biosensors - sensor principles and architectures. Sensors 8 (3), 1400–1458.

Gulati, P., Kaur, P., Rajam, M.V., Srivastava, T., Ali, M.A., Mishra, P., Islam, S.S., 2018. Leukemia biomarker detection by using photoconductive response of CNT electrode: analysis of sensing mechanism based on charge transfer induced Fermi level fluctuation. Sens. Actuators B Chem. 270, 45–55.

Herzog, G., Arrigan, D.W.M., 2005. Determination of trace metals by underpotential deposition–stripping voltammetry at solid electrodes. TrAC Trends Anal. Chem. 24 (3), 208–217.

Honeychurch, K.C., Hart, J.P., 2003. Screen-printed electrochemical sensors for monitoring metal pollutants. TrAC Trends Anal. Chem. 22 (7), 456–469.

Jie, G.F., Zhang, J., Jie, G.X., Wang, L., 2014. A novel quantum dot nanocluster as versatile probe for electrochemiluminescence and electrochemical assays of DNA and cancer cells. Biosens. Bioelectron. 52, 69–75.

Li, J., Zhang, Z., Rosenzweig, J., Wang, Y.Y., Chan, D.W., 2002. Proteomics and bioinformatics approaches for identification of serum biomarkers to detect breast cancer. Clin. Chem. 48 (8), 1296–1304.

Li, X.M., Liu, J.M., Zhang, S.S., 2010. Electrochemical analysis of two analytes based on a dual-functional aptamer DNA sequence. Chem. Commun. 46 (4), 595–597.

Liu, D.L., Zhuang, Q., Zhang, L., Zhang, H., Wu, S.Y., Kikuchi, J., Han, Z.B., Zhang, Q., Song, X.M., 2016. Self-assembly of novel fluorescent quantum dot-cerasome hybrid for bioelectrochemistry. Talanta 154, 31–37.

Liu, G.D., Wang, J., Kim, J., Jan, M.R., Collins, G.E., 2004. Electrochemical coding for multiplexed immunoassays of proteins. Anal. Chem. 76 (23), 7126–7130.

Liu, H., Xu, S., He, Z., Deng, A., Zhu, J.-J., 2013. Supersandwich cytosensor for selective and ultrasensitive detection of cancer cells using aptamer-DNA concatamer-quantum dots probes. Anal. Chem. 85 (6), 3385–3392.

Liu, W., Li, C., Tang, L., Tong, A., Gu, Y., Cai, R., Zhang, L., Zhang, Z., 2013. Nanopore array derived from L-cysteine oxide/gold hybrids: enhanced sensing platform for hydroquinone and catechol determination. Electrochim. Acta 88, 15–23.

Loren, A.W., Mangu, P.B., Beck, L.N., Brennan, L., Magdalinski, A.J., Partridge, A.H., Quinn, G., Wallace, W.H., Oktay, K., 2013. Fertility preservation for patients with cancer: american society of clinical oncology clinical practice guideline update. J. Clin. Oncol. 31 (19), 2500.

Ma, N., Sargent, E.H., Kelley, S.O., 2008. One-step DNA-programmed growth of luminescent and biofunctionalized nanocrystals. Nat. Nanotechnol. 4, 121.

Mullighan, C.G., Phillips, L.A., Su, X., Ma, J., Miller, C.B., Shurtleff, S.A., Downing, J.R., 2008. Genomic analysis of the clonal origins of relapsed acute lymphoblastic leukemia. Science 322 (5906), 1377–1380.

Mullighan, C.G., Su, X.P., Zhang, J.H., Radtke, I., Phillips, L.A.A., Miller, C.B., Ma, J., Liu, W., Cheng, C., Schulman, B.A., Harvey, R.C., Chen, I., Clifford, R.J., Carroll, W.L., Reaman, G., Bowman, W.P., Devidas, M., Gerhard, D.S., Yang, W.J., Relling, M.V., Shurtleff, S.A., Campana, D., Borowitz, M.J., Pui, C., Smith, M., Hunger, S.P., Willman, C.L., Downing, J.R., Childrens Oncology, G.,, 2009. Deletion of IKZF1 and prognosis in acute lymphoblastic leukemia. New Engl. J. Med. 360 (5), 470–480.

Pan, Y., Guo, M., Nie, Z., Huang, Y., Pan, C., Zeng, K., Zhang, Y., Yao, S., 2010. Selective collection and detection of leukemia cells on a magnet-quartz crystal microbalance system using aptamer-conjugated magnetic beads. Biosens. Bioelectron. 25 (7), 1609–1614.

Pitsillides, C.M., Runnels, J.M., Spencer, J.A., Zhi, L., Wu, M.X., Lin, C.P., 2011. Cell labeling approaches for fluorescence-based In vivo flow cytometry. Cytom. Part A 79A (10), 758–765.

Phillips, J.A., Xu, Y., Xia, Z., Fan, Z.H., Tan, W., 2009. Enrichment of cancer cells using aptamers immobilized on a microfluidic channel. Anal. Chem. 81 (3), 1033–1039.

Qian, H.F., Dong, C.Q., Weng, J.F., Ren, J.C., 2006. Facile one-pot synthesis of luminescent, water-soluble, and biocompatible glutathione-coated CdTe nanocrystals. Small 2 (6), 747–751.

Rowe, A.A., Chuh, K.N., Lubin, A.A., Miller, E.A., Cook, B., Hollis, D., Plaxco, K.W., 2011. Electrochemical biosensors employing an internal electrode attachment site and achieving reversible, high gain detection of specific nucleic acid sequences. Anal. Chem. 83, 9462–9466.

Saha, K., Agasti, S.S., Kim, C., Li, X.N., Rotello, V.M., 2012. Gold nanoparticles in chemical and biological sensing. Chem. Rev. 112 (5), 2739–2779.

Shao, Y., Wang, J., Wu, H., Liu, J., Aksay, I.A., Lin, Y., 2010. Graphene based electrochemical sensors and biosensors: a review. Electroanalysis 22 (10), 1027–1036.

Shen, Y., Li, X., Chen, W., Cheng, F., Song, F., 2013. Electrochemical determination of indole butyric acid by differential pulse voltammetry on hanging mercury drops electrode. J. Plant Biochem. Biotechnol. 22 (3), 319–323.

Singh, S.K., Hawkins, C., Clarke, I.D., Squire, J.A., Bayani, J., Hide, T., Henkelman, R.M., Cusimano, M.D., Dirks, P.B., 2004. Identification of human brain tumour initiating cells. Nature 432, 396.

Schamhart, D., Swinnen, J., Kurth, K.-H., Westerhof, A., Kusters, R., Borchers, H., Sternberg, C., 2003. Numeric definition of the clinical performance of the nested reverse transcription-PCR for detection of hematogenous epithelial cells and correction for specific mRNA of non-target cell origin as evaluated for prostate cancer cells. Clin. Chem. 49 (9), 1458.

Surmann, P., Zeyat, H., 2005. Voltammetric analysis using a self-renewable non-mercury electrode. Anal. Bioanal. Chem. 383 (6), 1009–1013.

Tu, W., Fang, X., Lou, J., Dai, Z., 2015. Label-free and highly sensitive electrochemiluminescence biosensing using quantum dots/carbon nanotubes in ionic liquid. Analyst 140 (8), 2603–2607.

Wang, J., Lu, J., Hocevar, S.B., Farias, P.A.M., Ogorevc, B., 2000. Bismuth-coated carbon electrodes for anodic stripping voltammetry. Anal. Chem. 72 (14), 3218–3222.

Wang, J., Wang, X., Tang, H., Gao, Z., He, S., Li, J., Han, S., 2018a. Ultrasensitive electrochemical detection of tumor cells based on multiple layer CdS quantum dots-functionalized polystyrene microspheres and graphene oxide – polyaniline composite. Biosens. Bioelectron. 100 (Supplement C), 1–7.

Wang, J., Wang, X., Tang, H., He, S., Gao, Z., Niu, R., Zheng, Y., Han, S., 2018b. A ratiometric magnesium sensor using DNAzyme-templated CdTe quantum dots and Cy5. Sens. Actuators B Chem. 272, 146–150.

Wang, J., Wang, X., Tang, H., Gao, Z., He, S., Ke, D., Zheng, Y., Han, S., 2017. Facile synthesis and properties of CdSe quantum dots in a novel two-phase liquid/liquid system. Opt. Mater. 72, 737–742.

Yang, Y., Fang, D., Liu, Y., Liu, R., Wang, X., Yu, Y., Zhi, J., 2018. Problems analysis and new fabrication strategies of mediated electrochemical biosensors for wastewater

toxicity assessment. Biosens. Bioelectron. 108, 82–88.
Yu, W.W., Qu, L.H., Guo, W.Z., Peng, X.G., 2004. Experimental determination of the extinction coefficient of CdTe, CdSe and CdS nanocrystals (vol 15, pg 2854, 2003). Chem. Mater. 16 (3) (560-560).
Zhang, H., Wang, D., Yang, B., Moehwald, H., 2006. Manipulation of aqueous growth of CdTe nanocrystals to fabricate colloidally stable one-dimensional nanostructures. J. Am. Chem. Soc. 128 (31), 10171–10180.
Zhang, K.Y., Lv, S.Z., Lin, Z.Z., Tang, D.P., 2017. CdS:Mn quantum dot-functionalized g-C3N4 nanohybrids as signal-generation tags for photoelectrochemical immunoassay of prostate specific antigen coupling DNAzyme concatamer with enzymatic biocatalytic precipitation. Biosens. Bioelectron. 95, 34–40.
Zhou, S., Wang, Y., Zhu, J.-J., 2016a. Simultaneous detection of tumor cell apoptosis regulators Bcl-2 and bax through a dual-signal-marked electrochemical immunosensor. Acs Appl. Mater. Interfaces 8 (12), 7674–7682.
Zhou, W., Li, C., Sun, C., Yang, X., 2016b. Simultaneously determination of trace $Cd^{2+}$ and $Pb^{2+}$ based on L-cysteine/graphene modified glassy carbon electrode. Food Chem. 192, 351–357.
Zhu, C.L., Lu, C.H., Song, X.Y., Yang, H.H., Wang, X.R., 2011. Bioresponsive controlled release using mesoporous silica nanoparticles capped with aptamer-based molecular gate. J. Am. Chem. Soc. 133, 1278–1281.